GENERALIZED RECONSTRUCTION BY INVERSION OF COUPLED SYSTEMS (GRICS) APPLIED TO PARALLEL MRI.

F. Odille[†]*, P.-A. Vuissoz, J. Felblinger*

Nancy University and INSERM ERI 13
Imagerie Adaptative Diagnostique et Interventionnelle
Nancy, France

D. Atkinson

University College London
Centre for Medical Image Computing
London, UK

ABSTRACT

This paper presents a framework allowing parallel MRI to be optimized. Parallel imaging relies on good coil sensitivity map estimates. As these sensitivities are determined experimentally, errors may occur during their assessment, whether using prior calibration (due to patient motion between calibration and actual scan), or autocalibration (due to lower resolution, suboptimal estimates). Here we reformulate reconstruction as a coupled inverse problem, consisting of simultaneously solving the parallel imaging problem, based on SENSE algorithm, and minimizing the propagation of sensitivity map errors in that reconstruction. The problem is practically solved using a multiresolution fixed-point iterative method, producing both the reconstructed image and optimized sensitivity maps. The method was validated by comparing sensitivity maps and reconstructed images obtained by standard SENSE reconstruction, based on a reduced number of autocalibration signal (ACS) data, to those obtained by the proposed method, starting from the same ACS data as initial guess.

Index Terms— Coupled problems, fixed-point iteration, magnetic resonance, recontruction, parallel imaging

1. INTRODUCTION

Parallel MRI relies on additional information provided by the spatial sensitivities of radiofrequency (RF) surface coil arrays in order to invert aliasing artifacts produced by undersampled k-space acquisition, below the Nyquist frequency [1]. This technique allows scan time to be reduced by a factor equal to the undersampling ratio. However there are several issues associated with the experimental determination of these coil sensitivities. A first approach consists of measuring them in a low resolution calibration scan, performed prior to the scan of interest. In practice, the computation may be affected by noise, and by regions in which no signal lies (division by zero), referred to as holes. Polynomial fitting and binary masks can be used [1] in order to overcome these difficulties, as well as methods inspired from image inpainting problems [2]. All parameters involved are thus optimal for the calibration scan, but may not be optimal for the scan of interest, due to patient motion in particular. This is one reason why alternative techniques, named autocalibrated, have been proposed recently [3, 4, 5]. These techniques are based on the acquisition of certain autocalibration signal (ACS) data, embodied in the pulse sequence of interest, allowing simultaneous acquisition of undersampled k-space data and coil sensitivities. A reduced number of ACS data should be used, otherwise the benefit of using parallel imaging, in terms of scan time reduction, is minimized. However using too few ACS data yields lower resolution, suboptimal sensitivity maps, and thereby may not completely invert aliasing artifacts.

It has been suggested recently that a reconstructed image (here, using the SENSE algorithm [1]) and coil sensitivities could be estimated jointly [6, 7]. Reconstruction is then reformulated as a large scale non-linear problem, consisting of optimizing a cost function (a quadratic criteria derived from the signal equation) with respect to two sets of parameters: the reconstructed image and the parameters describing coil sensitivities. Although the number of unknowns may be high and lead to an underdetermined system, one way to overcome the problem is, as proposed by the authors, to decouple the large-scale problem, by optimizing the cost function with respect to each set of parameters successively and iteratively, leading to two smaller (and better conditioned) problems.

This paper proposes to extend the latter method and address certain issues that may arise. Parallel imaging is reformulated in terms of two coupled inverse problems: image reconstruction (assuming known sensitivity maps) and minimization of sensitivity map error propagation (assuming known image). A model for sensitivity maps is introduced in order to solve the sensitivity map optimization problem. This model is similar to that proposed in [2], as it includes several constraints (smoothness and sum-of-squares consistency of the coil array). A multiresolution, fixed-point iterative method is then described for solving the coupled

*This work was funded by RNTS 2003 and Région Lorraine.
†The first author performed part of the work while at CMIC, London, funded by UK EPSRC E001564.

problem. The framework was tested on real data by comparing reference image and sensitivity maps, extracted from a fully sampled acquisition, to those obtained by the proposed method, using an undersampled dataset and a reduced number of ACS lines.

2. THEORY

2.1. Parallel Imaging Reconstuction

The general theory of parallel imaging was described in [1, 8]. Assuming coil sensitivity estimates are available, reconstruction of the image ρ from the k-space signal s can be seen as the inversion of the following signal equation, written in matrix formalism:

$$s = E\rho, \text{ with } \mathrm{E} = \begin{bmatrix} \xi F \mathrm{diag}(\sigma_1) \\ \vdots \\ \xi F \mathrm{diag}(\sigma_{\mathrm{N}_\gamma}) \end{bmatrix}, \tag{1}$$

where we used the following notations:
- ξ is the sampling operator ($0/1$ values in Cartesian case),
- F is the 2D/3D Fourier transform operator,
- $diag(\sigma_\gamma)$ is the γ^{th} coil sensitivity weighting operator.

It is possible to take into account noise correlation between coil elements by introducing a noise covariance matrix ψ. Writting $\psi = LL^H$, then the problem is still described by Eq. (1), after applying the substitutions $s := \{L^{-1} \otimes Id_{N_\gamma}\}s$ and $E := \{L^{-1} \otimes Id_{N_\gamma}\}E$, as shown in [8]. This amounts to working on virtual decorrelated receivers. In the remainder of this paper, we will assume that $\psi = Id$ in order to simplify notations, however taking into account noise correlation between receivers would be straight forward using this transformation.

2.2. Propagation of Coil Sensitivity Estimation Errors

Assuming an error $\delta\sigma = \{\delta\sigma_1 | \cdots | \delta\sigma_{N_\gamma}\}$ is made when determining sensitivity maps (using either prior sensitivity calibration or autocalibration), then the signal equation (1) is modified in the following manner:

$$s = E\rho + \varepsilon, \tag{2}$$

with ϵ being a reconstruction residue induced by this error. The residue expression is given below and can be rearranged:

$$\begin{aligned} \varepsilon &= \begin{bmatrix} \xi F \mathrm{diag}(\delta\sigma_1) \\ \vdots \\ \xi F \mathrm{diag}(\delta\sigma_{\mathrm{N}_\gamma}) \end{bmatrix} \rho \\ &= \begin{bmatrix} \xi F \mathrm{diag}(\rho) & & 0 \\ & \ddots & \\ 0 & & \xi F \mathrm{diag}(\rho) \end{bmatrix} \begin{bmatrix} \delta\sigma_1 \\ \hline \vdots \\ \hline \delta\sigma_{N_\gamma} \end{bmatrix} \\ &= R(\rho)\delta\sigma \end{aligned} \tag{3}$$

Equation (3) gives a theoretical expression describing sensitivity map error propagation. In particular, if a mask is applied to sensitivity maps, and if patient motion occurs, the misalignement will generate a $\delta\sigma$ composed of strong edges. Then the voxel-wise products $diag(\rho)\delta\sigma_\gamma$ will contain high spatial frequencies that will enter the Fourier operator, thus creating undesired ghost artifacts in the reconstructed image. Sensitivity maps having too low resolution will weight the voxel-wise products $diag(\rho)\delta\sigma_\gamma$ with intermediate spatial frequencies, which may modify the contrast.

2.3. Generalized Reconstruction by Inversion of Coupled Systems (GRICS)

We propose to optimize the description of coil sensitivities by inverting Eq. (3) in order to estimate and compensate the error $\delta\sigma$. Combining Eq. (1) and Eq. (3), the parallel imaging problem is reformulated in terms of two coupled inverse problems:

$$\begin{cases} s = E(\alpha)\rho & \text{SENSE reconstruction} \\ \varepsilon(\rho, \delta\sigma) = R(\rho)\delta\sigma & \text{Sensitivity optimization} \end{cases} \tag{4}$$

3. METHODS

3.1. Model for Coil Sensitivity Optimization

Inverting sytem (3) is not easy as it may be underdetermined, especially when using an high number of coil elements. Nevertheless not all these data are independent, and it is possible to introduce a model imposing several constraints on the solution sensitivity maps. We propose to use the model described in [2], although here our main optimization criteria is derived from Eq. (3) (data fidelity criteria). This model includes two constraints in addition to the data fidelity criteria. The first one is a smoothness term imposed on sensitivity maps. This term also allows sensititivity values to be extrapolated in areas containing holes. The second constraint forces the sum-of-squares of the coil element array to be equal to one. This enables us to remove one degree of freedom associated with the magnitude of these sensitivity values, and ensures a certain consistency of these maps with respect to signal homogeneity in the field of view. If D is the domain in which the data fidelity criteria is imposed (i.e. defined by a binary mask $\lambda_D(x)$), then sensitivity map optimization can be seen as minimizing the following functional:

$$\begin{aligned} E(\delta\sigma, \nabla\delta\sigma) &= \int_\Omega \lambda_D(x) |R(\rho,\sigma)\delta\sigma - \varepsilon|^2 dx \\ &+ \mu \int_\Omega |\nabla(\sigma + \delta\sigma)|^p dx \\ &+ \nu \int_\Omega \left(1 - \sqrt{\textstyle\sum_{\gamma=1}^{N_\gamma} |\sigma + \delta\sigma|^2}\right) dx \end{aligned} \tag{5}$$

The power term is set to $p = 2$ in our application for simplicity, corresponding to an isotropic diffusion constraint. The solution of Eq. (5) is achieved by writting Euler-Lagrange equations (see details in [2]). We propose however a slightly different implementation, as this process will be repeated iteratively (see section 3.2). At each iteration, we fix the nonlinear term arising from the Euler-Lagrange equation (from the sum-of-squares term) to the value obtained with results from the previous iteration. Therefore the computational complexity of the nonlinear problem is reduced significantly, and only two linear system solvers are called within the main fixed-point loop to solve problems (1) and (5).

Although the magnitude is constrained by the sum-of-squares term, a phase is left as a degree of freedom in the coupled problem, and it may be distributed to either the image or the sensitivity maps. Here we were interested in reconstructing the magnitude image. Therefore, once the solution determined, we applied the phase to the sensitivities, thus allowing comparison between the reference complex sensitivties and those obtained by the GRICS method.

3.2. Multiresolution Fixed-Point Iteration

We propose to solve the coupled system (4) by means of a fixed-point iterative method. Starting from an initial guess $\sigma^{(0)}$ of sensitivity maps, given by the ACS lines, the algorithm consists of successively solving each optimization problem individually, while other optimization parameters are fixed. Therefore a first image estimate $\rho^{(0)}$ is found by inversion of Eq. (1) using initial sensitivity map estimates. Then the reconstruction residue is evaluated by $\epsilon = E\rho^{(0)} - s$. The second inverse problem in (4) is solved using the minimization procedure (5), yielding an estimate $\delta\sigma^{(0)}$ of the error made on sensitivity maps. The model is finally updated: $\sigma^{(1)} = \sigma^{(0)} + \delta\sigma^{(0)}$. The next iteration is started using the updated model, and iterations are performed until a stopping condition is reached (e.g. ϵ stops decreasing). The two linear system inversions involved in each iteration were solved using the GMRES algorithm.

Nonlinear optimization problems are known to depend strongly on initialization. A question that arises is how well would such a method perform in the presence of a small amount of ACS data (e.g. yielding the worst initial guess). To address this issue, the afore mentioned fixed-point algorithm is performed inside a multiresolution loop. Hence, reduced problems are solved first, using only the most central data in k-space as inputs of the coupled problem. Reduce image and coil sensitivity maps are found first, and are interpolated before being used as initialization of the next resolution level. The starting resolution is chosen according to the number of ACS lines, as they provide the initial guess.

3.3. Validation on Subject Data

MRI data were acquired on a GE 1.5 T Signa scanner (General Electric, Milwaukee, WI), with an 8 element cardiac coil array. Cardiac data from two healthy volunteers were used. Imaging was achieved using an ECG triggered black-blood RARE pulse sequence (black blood FSE, 256x256 matrix, 1.4 mm pixel size, TE=35 ms, ETL=16, TI=650 ms), acquired in breath hold, and providing a short axis slice of the heart. The k-space acquisition was fully sampled, so that reference data as well as undersampled data could be reconstructed and compared.

Reference, high resolution sensitivity maps were extracted from the fully sampled k-space, using a central square of 64 (with windowing). Sensitivities were computed by pixel-wise division of each coil signal by the sum-of-squares reconstruction of all coil elements.

A reduced number of lines, again taken in the center of k-space, were also chosen as ACS lines. Then we retrospectively selected an undersampled subset of the k-space to apply parallel imaging reconstrutions, based on these ACS data. Several reconstructions were compared: first, a self-calibrated SENSE (SC-SENSE) reconstruction, based on the high resolution sensitivity maps, was used as reference; second, a SC-SENSE reconstruction, using raw sensitivity estimates given by ACS lines; third, the GRICS method, with raw sensitivity estimates given by ACS lines as initialization. Errors made on senstivity map estimates and on reconstructed images, compared to their respective references, were assessed by the normalized root mean squared error (NRMSE).

Table 1. Error in sensitivity maps and reconstructed image.

	$NRMSE(\sigma)$ (10^{-1})		$NRMSE(\rho)$ (10^{-4})	
ACS lines	SC-SENSE	GRICS	SC-SENSE	GRICS
Subject 1				
2	4.5	2.4	14.4	12.9
4	4.1	1.8	11.6	6.4
8	2.2	1.4	3.9	4.2
Subject 2				
2	4.4	2.5	16.2	8.4
4	4.2	2.0	13.3	6.3
8	2.2	1.8	5.0	4.8

4. RESULTS

Table 1 shows results obtained with SC-SENSE and with the proposed GRICS method. Both sensitivity maps and reconstructed images were improved with GRICS compared to using raw sensitivities obtained from ACS data. The best improvement was achieved when using 2 or 4 ACS lines, as they generated the worst sensitivity map estimates. Using 8 ACS lines, in these examples, was already enough to reconstruct an image without significant aliasing artifacts.

An example of such reconstruction results is also given in Fig. 1, with corresponding sensitivity maps in Fig. 2. In this example, the restriction to 4 ACS lines provided significant errors in sensitivity estimates, producing residual aliasing artifacts with a SC-SENSE method. The GRICS solution was able to improve both the sensitivity map estimate and the reconstructed image, and reduce residual artifacts using SC-SENSE.

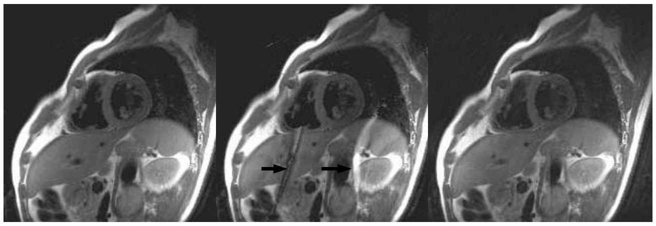

(a) (b) (c)

Fig. 1. Example parallel MRI reconstructions with a reduction factor of R=2: self-calibrated SENSE based on high resolution sensitivity maps (64 ACS lines) (a), self-calibrated SENSE using 4 ACS lines (b), and the proposed GRICS method using 4 ACS lines as initial guess (c).

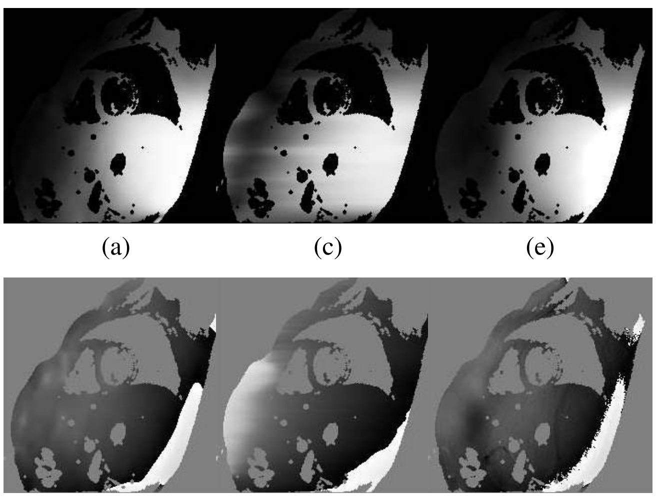

(a) (c) (e)

(b) (d) (f)

Fig. 2. Example sensitivity map (one coil, with binary mask applied for visualisation): high resolution sensitivity map (64 ACS lines) magnitude (a) and phase (b); low resolution map (4 ACS lines) magnitude (c) and phase (d); GRICS solution (4 ACS lines as initial guess) magnitude (e) and phase (f).

5. DISCUSSION AND CONCLUSIONS

In the GRICS framework, parallel imaging is reformulated as a coupled inverse problem. Its resolution, using a fixed-point method, allows both the coil sensitivity maps and the reconstructed image to be improved compared to using raw, low resolution coil sensitivity estimates. This approach could be applied to autocalibrated parallel imaging in order to reduce the number of ACS lines to embed in the pulse sequence of interest, which may be useful especially in 3D, or in fast dynamic imaging such as in k-t approaches.

However the proposed approach requires solving a large scale optimization problem, and hence may rely on good initialization. Here we proposed a multiresolution strategy in order to minimize this effect. We also proposed a relatively efficient implementation in terms of computation time, as fixed-point iterations involved in the solution of the nonlinear optimization problems (the large-scale problem (4) and the sensitivity map optimization (5)) were grouped into the same loop, inside which two linear problems are solved.

6. REFERENCES

[1] K. P. Pruessmann, M. Weiger, M. B. Scheidegger, and P. Boesiger, "SENSE: sensitivity encoding for fast MRI.," *Magn. Reson. Med.*, vol. 42, no. 5, pp. 952–962, Nov 1999.

[2] F. Huang, Y. Chen, G. R Duensing, J. Akao, A. Rubin, and C. Saylor, "Application of partial differential equation-based inpainting on sensitivity maps.," *Magn. Reson. Med.*, vol. 53, no. 2, pp. 388–397, Feb 2005.

[3] R. M. Heidemann, M. A. Griswold, A. Haase, and P. M. Jakob, "VD-AUTO-SMASH imaging.," *Magn. Reson. Med.*, vol. 45, no. 6, pp. 1066–1074, Jun 2001.

[4] M. A Griswold, P. M Jakob, R. M Heidemann, M. Nittka, V. Jellus, J. Wang, B. Kiefer, and A. Haase, "Generalized autocalibrating partially parallel acquisitions (GRAPPA).," *Magn. Reson. Med.*, vol. 47, no. 6, pp. 1202–1210, Jun 2002.

[5] C. A McKenzie, E. N Yeh, M. A Ohliger, M. D Price, and D. K Sodickson, "Self-calibrating parallel imaging with automatic coil sensitivity extraction.," *Magn. Reson. Med.*, vol. 47, no. 3, pp. 529–538, Mar 2002.

[6] L. Ying and J. Sheng, "Joint image reconstruction and sensitivity estimation in SENSE (JSENSE).," *Magn. Reson. Med.*, vol. 57, no. 6, pp. 1196–1202, Jun 2007.

[7] J. Sheng, L. Ying, E. W., and B. Liu, "Joint estimation of image and coil sensitivities in parallel spiral MRI," in *Biomedical Imaging: From Nano to Macro, 2007. ISBI 2007. 4th IEEE International Symposium on*. IEEE, 2007, pp. 133–136.

[8] K. P. Pruessmann, M. Weiger, P. Boernert, and P. Boesiger, "Advances in sensitivity encoding with arbitrary k-space trajectories.," *Magn. Reson. Med.*, vol. 46, no. 4, pp. 638–651, Oct 2001.